k dependence of the spin polarization in Mn_5Ge_3/Ge(111) thin films

W. Ndiaye,[1] J.-M. Mariot,[2,3] P. De Padova,[4] M. C. Richter,[1,5] W. Wang,[1,6,*] O. Heckmann,[1,5] A. Taleb-Ibrahimi,[7] P. Le Fèvre,[8] F. Bertran,[8] C. Cacho,[9] M. Leandersson,[10] T. Balasubramanian,[10] A. Stroppa,[11,12] S. Picozzi,[11,12] and K. Hricovini[1,5]

[1]*Laboratoire de Physique des Matériaux et des Surfaces, Université de Cergy-Pontoise, 5 mail Gay-Lussac, 95031 Cergy-Pontoise, France*

[2]*Sorbonne Universités, UPMC Univ Paris 06, UMR 7614, Laboratoire de Chimie Physique–Matière et Rayonnement, 11 rue Pierre et Marie Curie, F-75231 Paris Cedex 05, France*

[3]*CNRS, UMR 7614, Laboratoire de Chimie Physique–Matière et Rayonnement, 11 rue Pierre et Marie Curie, F-75231 Paris Cedex 05, France*

[4]*CNR, Istituto di Struttura della Materia, via Fosso del Cavaliere, 00133 Roma, Italy*

[5]*DSM, IRAMIS, Service de Physique de l'Etat Condensé, CEA-Saclay, 91191 Gif-sur-Yvette, France*

[6]*Institute of Precision Optical Engineering, School of Physics Science and Engineering, Tongji University, Shanghai 200092, People's Republic of China*

[7]*UR1-CNRS/Synchrotron SOLEIL, Saint-Aubin, B.P. 48, 91192 Gif-sur-Yvette Cedex, France*

[8]*Synchrotron SOLEIL, Saint-Aubin, B.P. 48, 91192 Gif-sur-Yvette Cedex, France*

[9]*Central Laser Facility, Rutherford Appleton Laboratory, Didcot, Oxon OX11 0QX, United Kingdom*

[10]*Lund University, MAX-lab, P.O. Box 118, 221 00 Lund, Sweden*

[11]*CNR, Institute for Superconducting and Innovative Materials and Devices (CNR-SPIN), 67100 L'Aquila, Italy*

[12]*Dipartimento di Fisica, Università degli Studi dell'Aquila, Via Vetoio 10, 67010 Coppito (L'Aquila), Italy*

(Received 21 October 2014; revised manuscript received 16 February 2015; published 11 March 2015)

Mn_5Ge_3(001) thin films grown on Ge(111) were studied by angle- and spin-resolved photoemission using synchrotron radiation in the 17–40 eV photon energy range. The photoelectron spectra were simulated starting from a first-principles band-structure calculation for the ground state, using the free-electron approximation for the final states, taking into account photohole lifetime effects and $k_\perp$ broadening plus correlation effects, but ignoring transition matrix elements. The measured spin polarizations for the various **k** points investigated in the ΓMLA plane of the Brillouin zone are found to be in fair enough agreement with the simulated ones, providing a strong support to the ground-state band-structure calculations. Possible origins for the departures between either simulations and experiments or previous and present experiments are discussed.

DOI: 10.1103/PhysRevB.91.125118 PACS number(s): 79.60.−i, 71.20.−b, 73.20.At

I. INTRODUCTION

Spintronics aims at adding the spin degree of freedom of the electron to the standard electronics, which relies only on the transport of the electrical charge. This opens the opportunity to develop new devices with enhanced functionalities (integration of logic and memory, nonvolatile functioning), increased speed, and reduced power consumption [1].

For the realization of such spintronic devices, it is important to consider materials that could be elaborated using the established Si-based technology. Such magnetic materials should ideally have a Curie temperature (T_C) above ambient temperature and a highly spin-polarized current. This is the reason why the intermetallic compound Mn_5Ge_3 has attracted a lot of attention. This ferromagnet is considered as a good candidate for spintronics as it can be grown epitaxially on Ge(111) and has a T_C of ≈290 K. To shed light on such a possibility, it is important to have detailed knowledge of the electronic structure of this material, namely the spin polarization at the Fermi level (E_F).

Theoretical investigations of the bulk electronic and magnetic properties of Mn_5Ge_3 have been performed using the density functional theory (DFT) [2–4]. They show a strong metallic character of Mn_5Ge_3 with a dominant Mn 3*d* contribution from E_F up to a binding energy (BE) of 3.5 eV.

On the experimental side, the spin-integrated electronic structure of Mn_5Ge_3 films grown on Ge(111) has recently been determined by angle-resolved photoelectron spectroscopy (ARPES) [5,6]. Due to the large photoionization cross section for Mn 3*d* electrons, a high photoelectron intensity is observed from E_F up to ≈3 eV BE. The nonvanishing spectral weight at E_F spreading out through the whole Brillouin zone (BZ) is attributed to flat minority-spin electron bands, almost parallel to the Fermi level, but contributions from other processes, requiring an approach beyond the one-electron picture, have to be taken into account as well: surface-perpendicular momentum ($k_\perp$) broadening, electron-electron interaction, and coupling of charge with bosonic degrees of freedom, such as phonons, polarons, and magnons [6].

Spin-resolved photoelectron spectroscopy (SRPES) measurements on Mn_5Ge_3(001)/Ge(111) films using $h\nu = 21.2$ eV photons have also been reported; they give a spin polarization P of $+(15 \pm 5)\%$ at E_F [7], in contrast to band-structure calculations (Ref. [2] and our calculations) where a negative polarization is obtained ($P = -41\%$). Thus the situation concerning the spin polarization in Mn_5Ge_3 is unclear.

In this paper, we report spin- and angle-resolved photoelectron spectroscopy (SARPES) measurements on Mn_5Ge_3(001)/Ge(111) films using synchrotron radiation. They allow to investigate in more detail the **k** dependence of the spin polarization, which constitutes a severe test of spin-polarized band-structure calculations. The experimental results are compared to simulations relying on calculations

*Present address: Department of Physics, Biology and Chemistry, Surface and Semiconductor Physics Group, Linköping University, SE-581 83 Linköping, Sweden.

 ©2015 American Physical Society

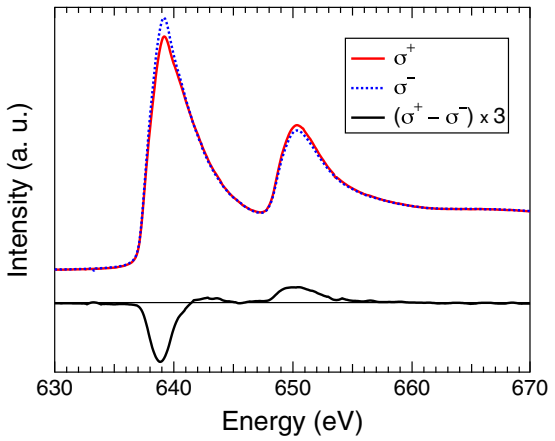

FIG. 1. (Color online) Mn $L_{2,3}$ x-ray absorption spectra measured for right- [σ^+ (red line)] and left-hand [σ^- (blue dashed line)] circularly polarized light and the corresponding ($\sigma^+ - \sigma^-$) XMCD signal (black line).

based on the DFT that have been demonstrated recently to be in very satisfactory agreement with ARPES data [6]. The trends of the **k** dependence of the spin polarization predicted by theory are found to follow closely the experimental observations.

II. EXPERIMENTAL AND COMPUTATIONAL DETAILS

The samples were prepared using the same procedure described in detail in Ref. [8]. The Mn_5Ge_3(001) thin films were grown on a Ge(111)-$c(2 \times 8)$ surface, prepared by cycles of sputtering (1 keV Ar^+ ions) of a Ge(111) substrate and annealing at 970 K until a sharp low-energy electron diffraction pattern was observed. Then 40–50 Mn monolayers were deposited from a Knudsen cell and the sample was annealed for several minutes at 720 K. This quantity of deposited Mn enables to build up a 200–270 Å thick Mn_5Ge_3 film. The structural characteristics of the samples were similar to those reported in Refs. [6] and [8].

The films were magnetized by applying a 900 gauss field *in situ* along the Ge[1$\bar{1}$0] direction, i.e., along the Mn_5Ge_3[100] direction. The efficiency of this procedure was established by measuring the Mn $L_{2,3}$ x-ray magnetic circular dichroism (XMCD). In Fig. 1, we show the x-ray absorption spectra at the Mn $2p$ edge for right- (σ^+) and left-hand (σ^-) polarized light and as well as the difference spectrum ($\sigma^+ - \sigma^-$). The measurements were done at 30 K with an angle of 45° between the photon beam and the sample magnetization. The XMCD spectra are in good qualitative agreement with those reported in the literature [9]. From a quantitative point of view, the relative amplitude of our XMCD signal, as compared to the published XMCD measurements [9], indicates that the magnetization of our samples was not completely saturated. This can have several origins and will be discussed in the next section.

Preliminary SARPES measurements were done at the I3 beamline of the MAX-lab synchrotron radiation center. But the series of SARPES results reported here were obtained at the Cassiopée beamline of the SOLEIL synchrotron radiation facility using a Scienta electron analyzer modified to allow spin

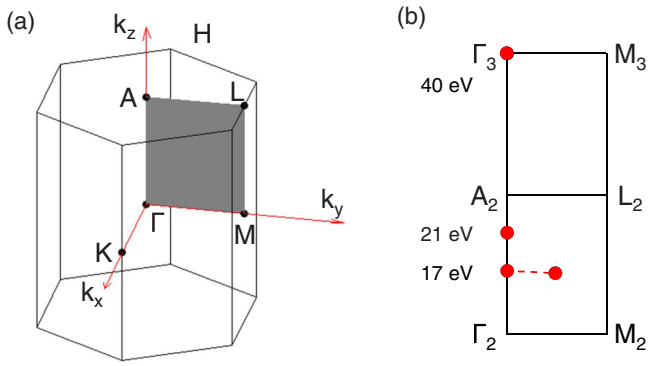

FIG. 2. (Color online) (a) Mn_5Ge_3 Brillouin zone with the ΓMLA plane indicated in grey. (b) **k**-space points investigated by SARPES (red dots) at normal emission for $h\nu = 17$, 21, and 40 eV and at 7° off-normal emission for $h\nu = 17$ eV.

analysis thanks to a Mott detector. In this setup, the angular acceptance of the analyzer is ≈±1.8°. The spectra were taken along the ΓA line of the Brillouin zone (BZ) and at one other point of the ΓMLA plane (see Fig. 2). All measurements have been performed with an overall energy resolution of 100 meV on samples in a remanent state held at 30 K.

The spin polarization P was calculated from the recorded intensities I for both magnetization directions (+/−) in two detector channels, L and R, by

$$P = \frac{1}{S} \frac{\sqrt{I_L^+ I_R^-} - \sqrt{I_R^+ I_L^-}}{\sqrt{I_L^+ I_R^-} + \sqrt{I_R^+ I_L^-}}, \quad (1)$$

where S is the Sherman function, determined to be 0.12 for the setup used here. Note that this experimental setup allows the determination of both the in-plane and the out-of-plane component of the spin vector in a single measurement.

The DFT calculations were performed using the Vienna Ab initio Simulation Package [10] within the generalized gradient approximation [11]. Projector augmented wave pseudopotentials [12,13] were used for both Ge and Mn atoms: the semicore $3p$ states are considered as valence (core) states for Mn (Ge); the $3d$ states are frozen in the core for Ge. The kinetic energy cutoff used for the wave functions was fixed to 350 eV. A $4 \times 4 \times 6$ Γ-centered **k**-point mesh was used for the self-consistent cycle. All the atomic internal positions were relaxed to minimize the *ab initio* stress and forces. The present calculations are mostly a recalculation of the band structure in order to allow a direct comparison to the present experimental data; they give almost identical results to those obtained in previous theoretical investigations of the electronic structure of Mn_5Ge_3 by some of us (see Refs. [2–4]).

Despite the very recent progress achieved in the one-step modeling of ARPES [14], such an approach remains, at present, out of scope for a complex system such as Mn_5Ge_3. So we did a simulation of the photoemission spectra using a simple model: the free-electron approximation for the final states was made, ignoring the matrix elements. In the simulation, the ground-state theoretical data were convoluted by Lorentzian and Gaussian functions to account for photohole lifetime effects and for $k_\perp$ broadening plus correlation effects,

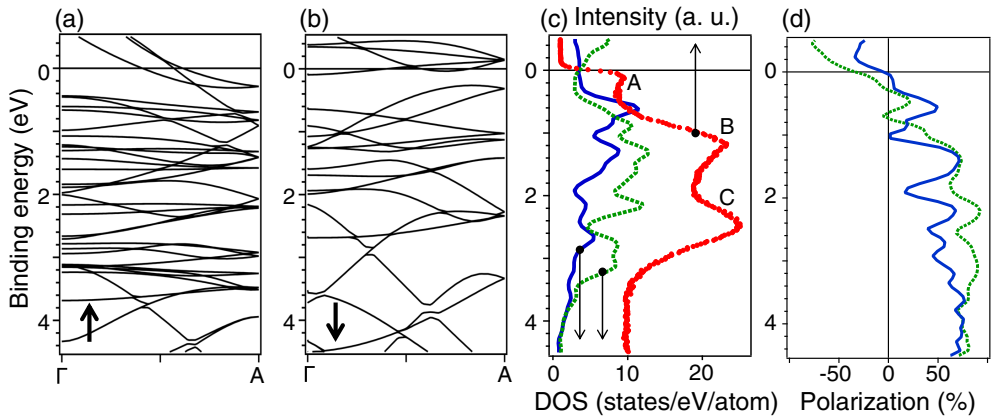

FIG. 3. (Color online) Mn_5Ge_3 calculated band structure for (a) majority and (b) minority electrons in the ΓA direction. (c) Spin-integrated normal emission spectrum at $h\nu = 17$ eV (red dots) and the Mn1 (blue line) and Mn2 (green dashed line) projected DOS for Mn 3*d* states. (d) Spin polarization calculated from the Mn1 (blue line) and Mn2 (green dashed line) projected DOS.

respectively. In a recent investigation [6], it has been shown that within such a model the ARPES spectra of Mn_5Ge_3 could be satisfactorily reproduced using Lorentzian broadening, with a full width at half maximum varying linearly from 0 at E_F to 1 eV at 8 eV BE, and a Gaussian broadening of 400 meV. The same set of parameters has been used here for consistency.

III. RESULTS AND DISCUSSION

In the complex crystalline structure of Mn_5Ge_3, there are two types of Mn sites, i.e., Mn1 atoms with six Ge neighbors at 2.53 Å and Mn2 atoms with five Ge neighbors (2, 1, and 2 at 2.48, 2.61, and 2.76 Å, respectively). The calculated majority- and minority-spin electronic states along the ΓA line are shown in panels (a) and (b), respectively, of Fig. 3, the photoelectron spectrum for $h\nu = 17$ eV (red dots) being shown in panel (c), where three main features (denoted A, B, and C) are observed. Main contributions to the photoelectron spectrum are expected from the high density of states (DOS) due to flat Mn 3*d* bands. It has been suggested [6] that, in a first step, we can determine the origin of these three features with the help of the Mn1 (blue line) and Mn2 (green dashed line) projected DOS [see Fig. 3(c)]. Consequently, feature B results mainly from Mn1 3*d* and Mn2 3*d* interaction and feature C is mostly due to Mn2 3*d* electrons. Feature A, in the vicinity of E_F, is built up by contributions resulting from hybridization between Mn1 and Mn2 3*d* electrons and between Mn 3*d* and Ge 4*p* electrons. Nonvanishing photoemission intensity at E_F is attributed to minority nondispersing bands [Fig. 3(b)] and, additionally, it can be generated by other processes, such as $k_\perp$ broadening and as well by a coupling of charge and bosonic (phonons, polarons, and magnons) degrees of freedom [6].

In line with the approximation mentioned above, it is interesting to consider the spin polarization originating from the projected DOS of Mn 3*d* states at both Mn1 (blue line) and Mn2 (green dashed line) sites, shown in panel (d) of Fig. 3. From this panel, it is seen that the overall spin polarization at E_F is predicted by the calculation to be negative, mainly due to Mn2 3*d* states. Above ≈0.5 eV BE, the polarization remains positive whatever the site. This global tendency is preserved in ARPES as detailed below. Namely, the overall negative spin polarization at E_F along the ΓA line is due to a minority band lying close to E_F.

We now turn more specifically to the discussion of our ARPES data. In Fig. 4(a), the spin polarization measured at normal emission for $h\nu = 21$ eV is given. This photon energy corresponds to a **k** point situated not far from the high symmetry point A on the ΓA line, as shown in Fig. 2(b). Both in-plane and out-of-plane spin polarizations are shown (in red and black, respectively). Note that the out-of-plane spin polarization is zero in the explored (0–3 eV) BE range. For the in-plane component, we observe a negative spin polarization at E_F and a large positive feature between 0.2 and 1.2 eV BE, which rises to ≈12%, together with two smaller features at

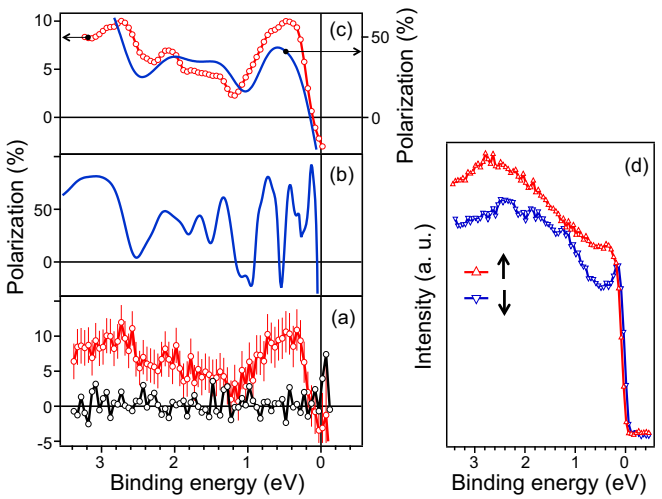

FIG. 4. (Color online) Valence-band spin polarization of Mn_5Ge_3(001). Measurements were done at normal emission with a photon energy of $h\nu = 21$ eV. (a) Spin polarization in the sample surface (red, with error bars) and perpendicular to the sample surface (black). (b) Spin polarization simulated taking into account the lifetime of the photohole. (c) Spin polarization simulated taking into account both lifetime and correlation effects (blue line), compared to the smoothed experimental in-plane spin polarization (red open dots). (d) Corresponding spin-resolved valence-band photoelectron spectra.

≈2 and 2.8 eV BE (with ≈7% and 11% of spin polarization, respectively). The simulation of the spin polarization obtained using the model described in the previous section is shown in Fig. 4(b) where only the photohole lifetime (Lorentzian) contribution is included. The additional convolution with a Gaussian distribution to include $k_\perp$ broadening and correlation effects reproduces very well the main features of the measured spectrum, as shown in Fig. 4(c) where the simulated spectrum (blue curve) is compared to the smoothed experimental spin polarization (red open dots). In Fig. 4(d), we show the spin-up $[I_\uparrow(E)]$ and spin-down $[I_\downarrow(E)]$ photoelectron spectra deduced from the spin polarization P and the spin-integrated spectrum $I(E)$ by

$$I_{\uparrow(\downarrow)} = \frac{I}{2}(1 \pm P)\,. \tag{2}$$

In the vicinity of E_F, where the photoemission intensity is not smeared out by the photohole lifetime broadening, the spectra are in very good agreement with calculations. As expected for the **k** point measured with the photon energy of $h\nu = 21$ eV [see Figs. 2(b), 3(a), and 3(b)] a minority peak is observed at E_F and the contribution of majority electrons is ≈0.3 eV below it.

The comparison between our measurement and the calculations reveals that the overall values of the measured spin polarization are smaller by a factor of ∼4–5 than those predicted by the simulation. This discrepancy can be qualitatively supported by the following arguments.

(i) In remanence, a Mn_5Ge_3 sample is not fully magnetized, because of the formation of magnetic domains. This is shown in Fig. 5 of Ref. [8] from which we deduce that we loose a factor of 1.3 in magnetization compared to the saturated magnetization. Moreover, taking into account the different temperatures, 30 K in our experiment and 245 K in the experiment presented in Ref. [9], as well as the angles between impinging photons and the magnetization vector, we obtain a factor of 2.6 in intensity reduction of our XMCD maximum signal due to unsaturated magnetization. Nevertheless, it should be kept in mind that, when the sample is not fully magnetized, the intensity of the measured signal is lowered, but the shape of the energy dependence of the spin polarization is not altered.

(ii) In nanometric ferromagnetic systems, the magnetic couplings at the surface can become highly frustrated, which can give birth to a magnetic dead layer (see, e.g., Ref. [15]). Thus it is quite probable that the outermost layer of our sample was nonmagnetic. Taking this fact into account and with an estimated mean free path for the photoelectrons of about 3 monolayers in Mn_5Ge_3, the external layer contributes 30% to the photoemission signal, diminishing the spin polarization by a factor of ≈1.5.

All the mentioned factors indicate the reduction in experimental spin polarization by a factor of ≈5, which, in fact, is close to the observations [see Fig. 4(c)]. In Figs. 5(b) and 5(c), one can remark a further decrease in spin polarization by about a factor of two with respect to that in Fig. 5(a). This is simply due to experimental conditions. As the spin-resolved experiments are time consuming and done at low temperature (see Sec. II), a thin layer of adsorbed residual gases is building up on the sample surface, attenuating the spin-polarized signal. As a matter of fact, the mentioned polarizations were measured

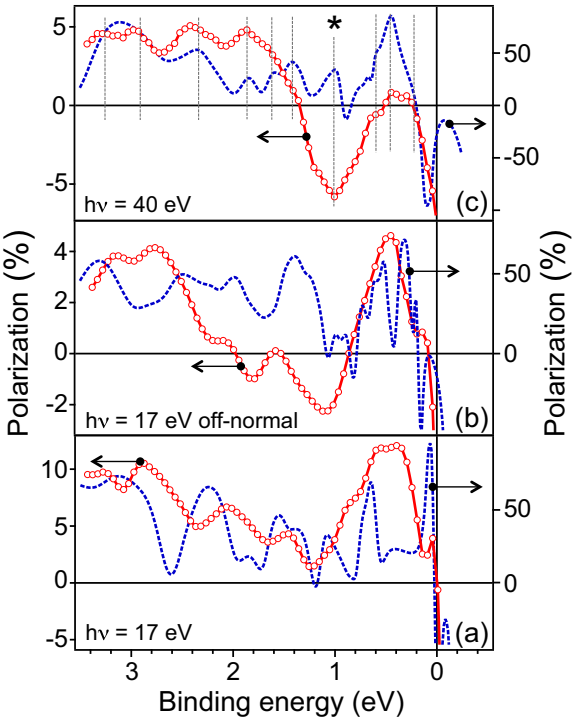

FIG. 5. (Color online) Spin polarization measured (red open dots) and simulated (blue dashed line) taking account the lifetime of the photohole for two normal emission spectra [(a) $h\nu = 17$ eV and (c) $h\nu = 40$ eV (corresponding to the Γ point of the BZ)] and one off-normal emission spectrum [(b) $\theta = 7^\circ$ and $h\nu = 17$ eV]. Vertical lines in (c) show the correspondence between experiment and simulation of different structures in the spectrum. See text for details.

at the end of the set of experiments. In addition to that, the limitations of our simplified model for spectral simulation have to be kept in mind when a comparison between experiment and theory is done.

In order to strengthen the agreement between the experiment and the theory, in Fig. 5, we compare experimental spin polarizations (red open dots) with simulations (blue dashed lines) for three other points of the BZ. Only the Lorentzian broadening accounting for the lifetime of the photohole is included in the simulation to allow a more detailed comparison with experiment because fine structures are not smeared out.

The spin polarization obtained in normal emission at $h\nu = 17$ eV [Fig. 5(a)] corresponds to a **k** point situated in the middle between Γ and A points. This is an interesting region of the BZ because, according to the band-structure calculations displayed in panels (a) and (b) of Fig. 3, the contribution of the spin-up bands to the spin polarization is counterbalanced by that from spin-down bands in the vicinity of E_F and an almost zero spin polarization is expected. In fact, this is in agreement with the observation. For BEs further below E_F, the density of electron bands is clearly higher for the majority spin, leading to a positive spin polarization, as observed in both measurements and simulations.

In Fig. 5(b), we show the spin polarization obtained with $h\nu = 17$ eV as well but moving out of normal emission ($\theta = 7^\circ$). The corresponding **k** point is situated in the middle of

the ΓMLA plane, away from high-symmetry lines and points. Again, the overall shape of the experimental spin polarization follows the calculated one; however, our simulation is unable to reproduce the negative polarization in the 1–2 eV BE range.

The normal emission spectrum measured with a photon energy of $h\nu = 40$ eV corresponds to the Γ point of the BZ and is shown in Fig. 5(c). Here, again, as in the preceding case [Fig. 5(b)], the sign of the polarization in the 0.5–1.2 eV BE range is not reproduced by the simulation. However, as already stressed, we used a simple model in our interpretation of the spectra, neglecting, namely, the matrix elements in the photoemission process. As a consequence, when simulating the spin polarization, each electron band has the same weight, which at some **k** points may lead to a wrong prediction of the spin polarization sign. One of these discrepancies is indicated in Fig. 5(c) by a vertical line with a five-pointed star at its top. Here, the simulation accurately predicts an extremum in the polarization, but with an opposite sign.

In this context, one can qualitatively argue that the discrepancies might by due to the different origin of electrons influencing photoemission matrix elements. As mentioned above, electrons close to 1 eV BE result mainly from Mn1 3*d* and Mn2 3*d* interaction, whereas in the vicinity of the Fermi level Mn 3*d* and Ge 4*p* electrons are hybridized [2]. Moreover, for BE of about 1 eV, the calculated spin polarizations [see Fig. 3(d) for global behavior] exhibit deep minima and values close to zero. Consequently, the sign in the polarization, as determined in the experiment, is very sensitive to the matrix elements. At the Fermi level, the tendency for both, experiment and calculations, is rather to enhance the negative value of the spin polarization upon decreasing electron BE and crossing the Fermi level.

In spite of these facts, our results illustrate the power of spin-resolved photoemission that can reveal much finer details of the electronic structure than spin-integrated measurements. The vertical lines in Fig. 5(c) indicate that in the whole spectrum the correspondence of different structures between the experiment and simulation is really astonishing. These structures mark the presence of majority (minority) electron bands, because in these points the polarization is peaking or changing in slope, confirming thus the ground-state band calculations.

Prior to our measurements, Dedkov *et al.* [7] have reported one set of SRPES data on Mn_5Ge_3. Our monocrystal has a comparable thickness to that used in Ref. [7], and it exhibits the same properties as testified by our x-ray absorption spectra and the temperature-dependent magnetization measurements (see Ref. [8]). However, a difference appears between the photoemission measurements where the attribution of spin-up and spin-down spectra is reversed. Our minority electron spectrum has a pronounced peak at E_F, contrary to the corresponding spectrum in Ref. [7]. Logically, this is a consequence of the opposite sign of the spin polarization at E_F. A possible origin of this discrepancy might be attributed to the difference in the experimental configurations: the angular acceptance in Ref. [7] was 12° whereas it is ≈3.6° in our experiment. Nevertheless, our simulation of the spectrum including the angular acceptance of 12° leads again to the negative sign of the spin polarization at E_F. Although both experiments have been done with the same photon energy, drawing a definitive conclusion on this point is difficult.

IV. CONCLUSIONS

We have performed spin- and angle-resolved photoelectron spectroscopy measurements on Mn_5Ge_3(001)/Ge(111) thin films in the ΓMLA plane of the Brillouin zone. The experimental results are compared to simulations relying on spin-polarized band-structure calculations. The trends of the **k** dependence of the spin polarization predicted by theory are found to follow the experimental observations.

ACKNOWLEDGMENTS

The research leading to these results has received funding from the European Community's Seventh Framework Programme (FP7/2007-2013) under grant agreement No. 226716. We acknowledge the CINECA award under the ISCRA initiative, for the availability of high performance computing resources and support. Computational resources from the CASPUR supercomputing center (Rome) are also acknowledged.

[1] See, for instance, J. Sinova and I. Žutić, New moves of the spintronics tango, Nat. Mater. **11**, 368 (2012).

[2] S. Picozzi, A. Continenza, and A. J. Freeman, First-principles characterization of ferromagnetic Mn_5Ge_3 for spintronic applications, Phys. Rev. B **70**, 235205 (2004).

[3] A. Stroppa and M. Peressi, Non-collinear magnetic states of Mn_5Ge_3 compound, Mater. Sci. Semicond. Proc. **9**, 841 (2006).

[4] A. Stroppa and M. Peressi, Competing magnetic phases of Mn_5Ge_3 compound, Phys. Status Solidi A **204**, 44 (2007).

[5] J. H. Grytzelius, H. M. Zhang, and L. S. O. Johansson, Surface atomic and electronic structure of Mn_5Ge_3 compound on Ge(111), Phys. Rev. B **84**, 195306 (2011).

[6] W. Ndiaye, M. C. Richter, O. Heckmann, P. De Padova, J.-M. Mariot, A. Stroppa, S. Picozzi, W. Wang, A. Taleb-Ibrahimi, P. Le Fèvre, F. Bertran, C. Cacho, M. Leandersson, T. Balasubramanian, and K. Hricovini, Bulk electronic structure of Mn_5Ge_3/Ge(111) films by angle-resolved photoemission spectroscopy, Phys. Rev. B **87**, 165137 (2013).

[7] Yu. S. Dedkov, M. Holder, G. Mayer, M. Fonin, and A. B. Preobrajenski, Spin-resolved photoemission of a ferromagnetic Mn_5Ge_3(0001) epilayer on Ge(111), J. Appl. Phys. **105**, 073909 (2009).

[8] P. De Padova, J.-M. Mariot, L. Favre, I. Berbezier, B. Olivieri, P. Perfetti, C. Quaresima, C. Ottaviani, A. Taleb-Ibrahimi, P. Le Fèvre, F. Bertran, O. Heckmann, M. C. Richter, W. Ndiaye, F. D'Orazio, F. Lucari, C. M. Cacho, and K. Hricovini, Mn_5Ge_3 films grown on Ge(111)-$c(2 \times 8)$, Surf. Sci. **605**, 638 (2011).

[9] L. Sangaletti, E. Magnano, F. Bondino, C. Cepek, A. Sepe, and A. Goldoni, Interface formation and growth of ferromagnetic

thin layers in the Mn:Ge(111) system probed by dichroic soft x-ray spectroscopies, Phys. Rev. B **75**, 153311 (2007).

[10] P. Blaha, K. Schwarz, G. K. H. Madsen, D. Kvasnicka, and J. Luitz, WIEN2K, *An Augmented Plane Wave + Local Orbitals Program for Calculating Crystal Properties* (K. Schwarz, Techn. Univ. Wien, 2001).

[11] J. P. Perdew, K. Burke, and M. Ernzerhof, Generalized gradient approximation made simple, Phys. Rev. Lett. **77**, 3865 (1996).

[12] P. E. Blöchl, Projector augmented-wave method, Phys. Rev. B **50**, 17953 (1994).

[13] G. Kresse and D. Joubert, From ultrasoft pseudopotentials to the projector augmented-wave method, Phys. Rev. B **59**, 1758 (1999).

[14] J. Braun, J. Minár, S. Mankovsky, V. N. Strocov, N. B. Brookes, L. Plucinski, C. M. Schneider, C. S. Fadley, and H. Ebert, Exploring the XPS limit in soft and hard x-ray angle-resolved photoemission using a temperature-dependent one-step theory, Phys. Rev. B **88**, 205409 (2013).

[15] Ji Ma and Kezheng Chen, Magnetic dead layer is not "magnetically dead" in hematite nanocubes, Phys. Lett. A **377**, 2216 (2013).